Electrochemistry Communications 50 (2015) 28–31

Contents lists available at ScienceDirect

Electrochemistry Communications

journal homepage: www.elsevier.com/locate/elecom

Synthesis of efficient Vulcan–$LaMnO_3$ perovskite nanocomposite for the oxygen reduction reaction

Gwénaëlle Kéranguéven [a,*], Sébastien Royer [b], Elena Savinova [a]

[a] ICPEES UMR7515-CNRS-Université de Strasbourg, 25 rue Becquerel, F-67087 Strasbourg Cedex 2, France
[b] IC2MP UMR7285-CNRS-Université de Poitiers, 4 Rue Michel Brunet, F-86022 Poitiers Cedex, France

ARTICLE INFO

Article history:
Received 22 October 2014
Accepted 31 October 2014
Available online 8 November 2014

Keywords:
Perovskite–carbon nanocomposite
Oxygen reduction reaction
Rotating disc electrode
In situ autocombustion synthesis

ABSTRACT

In situ autocombustion has been developed as a novel and efficient route for the synthesis of perovskite–carbon nanocomposites for the oxygen reduction reaction (ORR) in alkaline media. We demonstrate the synthesis of crystalline $LaMnO_{3+\delta}$ perovskite–Vulcan composite with a high accessibility of active sites and high electronic conductivity required for efficient electrocatalysis. The rotating disc electrode measurements evidenced an excellent activity of the composite for the ORR.

1. Introduction

The oxygen reduction reaction (ORR), which is largely responsible for the voltage losses in proton exchange fuel cells (PEMFC), is an enabling process for this attractive technology [1]. State-of-the-art electrocatalysts for the ORR are based on Pt group metals, whose high price and limited resources hamper the PEMFC commercialization. Transition metal oxides from the perovskite family were proposed as catalysts for the ORR and for the oxygen evolution reaction as a low cost substitute of noble metals already in the 1970s, and are currently attracting an increasing attention [2–8]. The perovskite structure can accommodate various cations, resulting in widely variable surface and bulk properties [9]. However, the major inconvenience of perovskites for electrocatalysis is their low specific surface area, ensuing from the high temperature required for the perovskite phase crystallization, and rarely exceeding 15–20 $m^2\ g^{-1}$ [9]. Even if recent advancements in the preparation of nanoperovskites [10,11] allowed to decrease the crystallite size to ≤15 nm, unsupported perovskites still show low surface areas resulting from the crystallite agglomeration. Moreover, it has been demonstrated that perovskites alone show low electrocatalytic activity [4–7], which may be increased by orders of magnitude when carbon is added to the catalytic layer. It has been shown that carbon in perovskite–carbon composites plays a dual role [5,6] by (*i*) improving the electronic conductivity of the catalytic layer, and (*ii*) by acting as a catalyst of the O_2 reduction to H_2O_2 (the latter further reacting to water on the oxide) [5,6]. Furthermore, Fabbri et al. inferred a synergetic chemical coupling between perovskite and carbon [7]. Until now, preparation of electrodes relies on the manual mixture of perovskites with carbon. Considering the important role of carbon, there is an urgent need for novel approaches towards the design of perovskite–carbon nanocomposites minimizing the size of oxide crystallites, the degree of their agglomeration, and maximizing the contact between oxide and carbon particles for efficient ORR electrocatalysis.

In this study, we propose in-situ autocombustion as an approach for dispersing perovskite crystallites in the carbon matrix and ensuring high accessibility of active sites and high electronic conductivity required for efficient electrocatalysis [12]. In the past in situ autocombustion was used for dispersing oxides over silica [13], but not on carbon. This work demonstrates preparation of pure perovskite–carbon composites with an excellent ORR activity.

2. Materials and methods

2.1. Material preparation

Unsupported $LaMnO_{3+\delta}$ was prepared following two routes, named autocombustion (LaMn-AC) and sol–gel (LaMn-SG). For LaMn-SG, La and Mn nitrates were used in 1:1 stoichiometry. The sample was annealed in air at 650 °C for 1 h, and milled in a planetary mill using WC balls in the presence of ethanol for 3 h at 120 rpm. For more details see Ref. [14]. For LaMn-AC, 0.18 g of $La(NO_3)_3 \cdot 6H_2O$ and 0.10 g of $Mn(NO_3)_2 \cdot 4H_2O$ were dissolved in 10 mL Milli-Q water. After 1 h, 0.16 g of glycine was added as a complexing agent. The solution was mixed for 1 h, water evaporated at 100 °C and the temperature was increased up to 300 °C to initiate glycine autoignition. Then the solid was calcined at 640 °C for 4 h under air, ensuring the formation of a pure perovskite phase and the removal of carbonaceous residues. For the

* Corresponding author. Tel.: +33 368852634; fax: +33 549453580.
E-mail address: kerangueven@unistra.fr (G. Kéranguéven).

http://dx.doi.org/10.1016/j.elecom.2014.10.019
1388-2481/

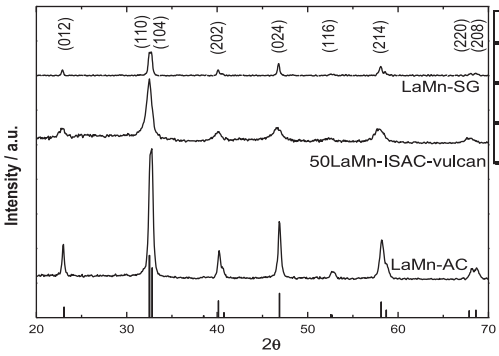

Sample	D_{XRD} [a] / nm	S_{BET} / $m^2 g^{-1}$	Pore size[c] / nm	Perovskite %[d]
LaMn-AC	25	17	42	
LaMn-SG	54	14	33	
50LaMn-ISAC-vulcan	8	76 [b]	21	50

[a] calculated by Scherrer equation with the shape factor K = 0.89
[b] value for the perovskite and carbon in composite
[c] mean pore size, evaluated by the B.J.H. method applied to the desorption branch, for the perovskite and carbon in composite
[d] % of oxide in composites obtained by TGA analysis, average of 3 measurements

Fig. 1. XRD for perovskite-based materials, vertical bars: ICCD card n°050-0298. The table summarizes structural and textural properties of materials: crystal size (XRD), specific surface area (BET) and mean pore size (B.J.H.), and perovskite weight % (TGA).

nanocomposite preparation via in situ autocombustion (ISAC) route, 0.1 g of Vulcan–XC72 carbon was added to the nitrate–glycine complex after 1 h before initiating the glycine autoignition. The solid was calcined at 350 °C for 30 min, which was sufficient for the formation of a well crystallized perovskite phase. The name of the composite (50LaMn–ISAC–Vulcan) bears the weight % of $LaMnO_3$ (50%), the type of the synthesis (ISAC) and of carbon (Vulcan).

2.2. Material characterization

The structure of synthesized materials was evaluated by X-ray diffraction (XRD) using D8 Advance Brucker diffractometer equipped with a copper anticathode using the Kα1 radiation. Morphology of the samples was determined by Transmission Electron Microscopy (TEM) and Scanning Electron Microscopy (SEM). The surface area was measured by N_2-physisorption at 77 K, applying the Brunauer–Emmett–Teller (BET) model. For 50-LaMn–ISAC–Vulcan there is no direct access to the specific surface area of the oxide, because its BET surface area (Fig. 1) corresponds to the sum of the contributions of carbon and perovskite. Finally, the weight% of perovskite in 50-LaMn–ISAC–Vulcan was determined by thermogravimetry analysis (TGA) conducted under the air flow of 25 mL min^{-1}, from 25 to 1000 °C at a heating rate of 10 °C min^{-1}.

2.3. Electrochemical measurements

For the working electrode preparation, catalyst powders (ISAC nanocomposite and perovskite manually mixed with carbon) were mixed with Milli-Q water, and an aliquot of this suspension was drop-casted onto the GC insert of a rotating disc electrode (RDE, 0.19 cm^2) to obtain 46 μg cm^{-2} oxide loading. The loading of Vulcan-XC72 electrode was 37 μg cm^{-2}. After drying under N_2, AS-4-ionomer was added as a binder to improve the film stability. The electrochemical measurements were performed in a Teflon cell comprising a platinum wire counter and the Hg/HgO/1 M NaOH reference electrode in 1 M NaOH using Autolab potentiostat at 10 mVs^{-1} and 25 °C. For further details see Ref. [5].

3. Results

Structural data are shown in Fig. 1. XRD confirms formation of the $LaMnO_{3+\delta}$ perovskite phase (ICDD card n°050-0298) with a comparable content of Mn^{4+} for all materials synthesized in this work. Despite the fact that only the perovskite phase was detected by the XRD, formation of other species (like single oxides or carbides) in small amounts at the interface between the oxide and carbon cannot be completely excluded. The $LaMnO_{3+\delta}$ crystallite size estimated using Scherrer equation decreases from 54 nm for the SG to 25 nm for the AC, and down to 8 nm for the ISAC method. The smaller size of the oxide crystallites for 50-LaMn–ISAC–Vulcan vs. LaMn-AC and LaMn-SG is likely to originate from its lower calcination temperature and from the presence of carbon which may act as a crystal growth inhibitor.

Fig. 2 shows representative TEM and SEM images of $LaMnO_{3+\delta}$ prepared by various routes. In agreement with the XRD data, SEM and TEM confirm formation of smaller oxide particles via AC (25–50 nm, Fig. 2A, B) compared to the SG (50–100 nm, Fig. 2C,D) synthesis, which unfortunately only leads to a marginal increase in the BET surface area from

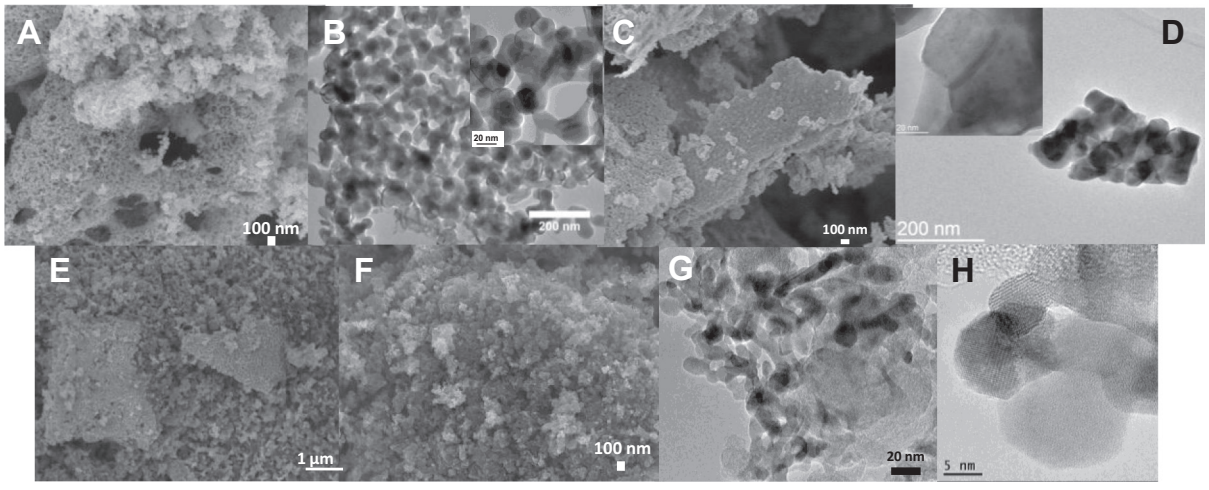

Fig. 2. Images recorded by: SEM (A) and TEM (B) for LaMn-AC; SEM (C) and TEM (D) for LaMn-SG; SEM (E) for LaMn-AC manually mixed with Vulcan–XC72 in 1:1 mass ratio; and SEM (F) and TEM (G, H) for 50-LaMn–ISAC–Vulcan.